Open Journal of Marine Science, 2023, 13, 41-65
https://www.scirp.org/journal/ojms
ISSN Online: 2161-7392
ISSN Print: 2161-7384

Hydrodynamic Performance of a Newly-Designed Pelagic and Demersal Trawls Using Physical Modeling and Analytical Methods for Cameroonian Industrial Fisheries

Tcham Leopold[1], Vanlie Maurice Kontchou[1], Nyatchouba Nsangue Bruno Thierry[1,2*], Abdou Njifenjou[1], Njomoue Pandong Achille[1*]

[1]Laboratory of Energy, Materials, Modeling and Method (E3M), National Higher Polytechnic School of Douala, University of Douala, Douala, Cameroon
[2]College of Marine Science, Shanghai Ocean University, Shanghai, China
Email: *nnbt@shou.edu.cn, *njopanac@hotmail.com

How to cite this paper: Leopold, T., Kontchou, V.M., Thierry, N.N.B., Njifenjou, A. and Achille, N.P. (2023) Hydrodynamic Performance of a Newly-Designed Pelagic and Demersal Trawls Using Physical Modeling and Analytical Methods for Cameroonian Industrial Fisheries. *Open Journal of Marine Science*, **13**, 41-65.
https://doi.org/10.4236/ojms.2023.133004

Received: March 27, 2023
Accepted: July 4, 2023
Published: July 7, 2023

Abstract

This study proposed the newly-designed Pelagic and demersal trawls for the fishing vessels operating in Cameroonian waters in pelagic and demersal fishing grounds. The engineering performances of both trawls were investigated using physical modelling method and analytical method based on the predicted equations. In a flume tank, a series of physical model tests based on Tauti's law were performed to investigate the hydrodynamic and geometrical performances of both trawls and to assess the applicability of the analytical methods based on predicted equations. The results showed that in model scale, the working towing speed and door spread for the pelagic trawl were 3.5 knots and 1.85 m, respectively, and for the bottom trawl net they were 4.0 knots and 1.8 m. At that speed and door spread, the drag force, net opening height, and wing-end spread of the pelagic model trawl were 36.73 N, 0.89 m, and 0.86 m, respectively, and the swept area was 0.76 m^2. Bottom trawl speed and door spread were 30.43 N, 0.38 m, and 0.45 m, respectively, and the swept area was 0.25 m^2. The maximum difference between the experimental and analytical results of hydrodynamic performances was less than 56.22% and 41.45%, respectively, for pelagic and bottom trawls, the results of the geometrical performances obtained using predicted equations were close to the experimental results in the flume tank with a maximum relative error less than 12.85%. The newly developed pelagic and bottom trawls had advanced engineering performance for high catch efficiency and selectivity and could be used in commercial fishing operations in Cameroonian waters.

Keywords

Cameroonian Waters, Pelagic Trawl, Bottom Trawl, Engineering Performances, Physical Model Test, Analytical Methods Formatting

1. Introduction

Cameroon's exclusive economic zone is located at the latitude of 3˚27'46" N (3.46278°) and the longitude of 9˚18'39.2" E (9.31089°) in the Gulf of Guinea. This area is part of eastern tropical Atlantic Ocean of the West African coast, extending west from Cape Lopez near the equator, to Cape Palmas at longitude 7° west. Thus, the Cameroonian coastline stretches for about 400 Km along the Atlantic Ocean with a stretch from the border with Equatorial Guinea, south of the Campo River estuary (2˚20'N) to at the Nigerian border north of the Akwayafe River (4˚40'N). However, the Cameroonian's industrial and semi industrial fishing are dominated by pelagic fish such as Clupeidae as clupea harengus, Sardina pilchadus, Sardinella maderensis, Ethmolosa fimbriata, Illisha Africana, pseudotolithus senegalensis, pseudotolithus typus Parapenaeopsis atlantica, Penaeus kerathurus, Ethmalosa fimbriata; Sardinella maderensis; Pseudotolithus elongatus; Pseudotolithus senegalensis; Pseudotolithus typus; Chloroscumbus chrysurus, Penaeus monodon, cynoglossus canariensis, and dasyatis garouensis [1] [2]. Thus, this fishing has traditionally been conducted using pelagic and bottom trawl technologies that are towed about four times a day with about six tonnes of fish being caught in each trawl [1] [3] [4] [5] [6]. The trawl nets used in the Cameroonian fishery differ in design and mesh configuration. Some trawls have small meshes throughout the trawl such as shrimp trawl, while other trawl designs have large meshes in the mouth area with successive reductions in the trawl panels towards the small meshed codend in the case of the demersal and pelagic trawl [7].

However, there are numerous obstacles, particularly for the trawl fisheries in Cameroonian water, which are under tremendous pressure to increase energy efficiency during fishing operations due to the continuous increase in fuel price and decrease in fish stocks [8] [9]. Therefore, as a result, higher resource utilization, the best structural design of the trawl is required to reduce hydrodynamic force, reduce by-catch, increase juvenile escape rate, high energy efficiency, and reduce environmental effect from the fishing operation would be benefits of the trawl's design and performance [6]. Indeed, the drag and the sweep area during fishing operations have a significant impact on the energy efficiency of trawl nets. Therefore, the twine diameter can be decreased, the mesh size increased, or square meshes used, twine material replaced with Dyneema and nylon monofilament, and the shape of the trawl net and door spread modified [5] [6] [10]. The ratio of drag to swept area must be minimized, nevertheless, in order to optimize catchability. Therefore, increasing the geometrical shape of the trawl system, such as wing-end spread and net mouth opening, is one of the solutions. Increasing the door spread (trawl door opening) and buoyancy can help achieve it.

In order to improve fuel consumption by reducing net drag, the dynamic behavior of trawl nets has been investigated for decades using theoretical, experimental, and numerical modeling methods [8] [11] [12] [13]. The evaluation of new trawl designs using physical models in a flume tank has become the de facto norm, and it is a crucial step in the process of developing modern gear [14] [15]. The geometry and hydrodynamic resistance of the Canadian demersal survey trawl (Campelen 1800) were compared using dynamic simulation, flume tank testing, and full-scale at-sea observations. By testing the model nets in the flume tank, Lee *et al.* [8] recommended novel designs of midwater trawl and trawl doors to decrease fuel consumption in fisheries. In order to assess the degree of the combined trawl system drag reduction using flume tank tests and sea trials [10], examined the engineering performances of the commercial prawn trawls built from a variety of traditional and high-strength netting materials in conjunction with otter boards of three sizes. They discovered that the enhanced twine flexibility and increased flow passage through the trawl caused an increase in catch efficiency for larger, more mobile prawns, leading to the high-strength netting trawls catching larger prawns in comparison to the conventional Polyethylene trawl. By using numerical simulation and physical model tests, Wan *et al.* [13] designed and evaluated the hydrodynamic performance of a large Antarctic krill trawl (midwater trawl), concluding that the trawl with a large net opening circumference had a greater hydrodynamic performance and could be well matched with fishing vessels of the class for the effective production of Antarctic krill. For coastal fisheries, Nyatchouba *et al.* [5] [6] recently evaluated the impact of mesh size, twine thickness, and material on trawl performance and the prediction of full-scale at-sea performance of the bottom trawl net.

The present study aims to propose a new design of both pelagic trawl net and bottom trawl net in order improve the performance of Cameroonian fisheries. Thus, we examine the effect of door spread and flow velocity on the drag and net mouth height of the two trawl nets using model scale in the flume tank and analytical method based on the published equations develop by some researchers using experimental data. The findings are expected to contribute to the improvement of trawl performance currently employed in the Cameroonian industrial fishery.

2. Materials and Methods

2.1. Design of the Pelagic and Bottom Trawl Nets

The A new bottom trawl (86.1 × 46.5 m) and pelagic trawl net (300 m × 132.8 m (headline 55.68 m)) were designed for the target trawler using in Cameroonian water. The two trawl nets included four panels with diamond mesh designed from the Dyneema. A 1:35 scale (λ = 15) and 1:20 scale (λ = 20) for midwater and bottom trawl, respectively, ratio of the total scale of the trawl model of the both trawls were manufactured based on modified Tauti's law developed by Hu *et al.* 2001 [16]. The pelagic trawl net was constructed from 6.0 mm and 4.0 mm diameter varying in mesh size from 400 mm the wing and the first body section to 200 mm in second to seventh body sections, and 144 mm in the remaining trawl body sections and the codend. While, the bottom trawl was constructed with a twine diameter varying from 2.6 to 3.82 mm and a mesh size varying from 240 mm in the trawl wing, 180 mm in the square, 120 mm in the first belly, 75 mm on other part of belly, and 60 mm on the codend (**Figure 1**). Main specifications and parameters of the full-scale trawl and the model trawls are provided in **Table 1**.

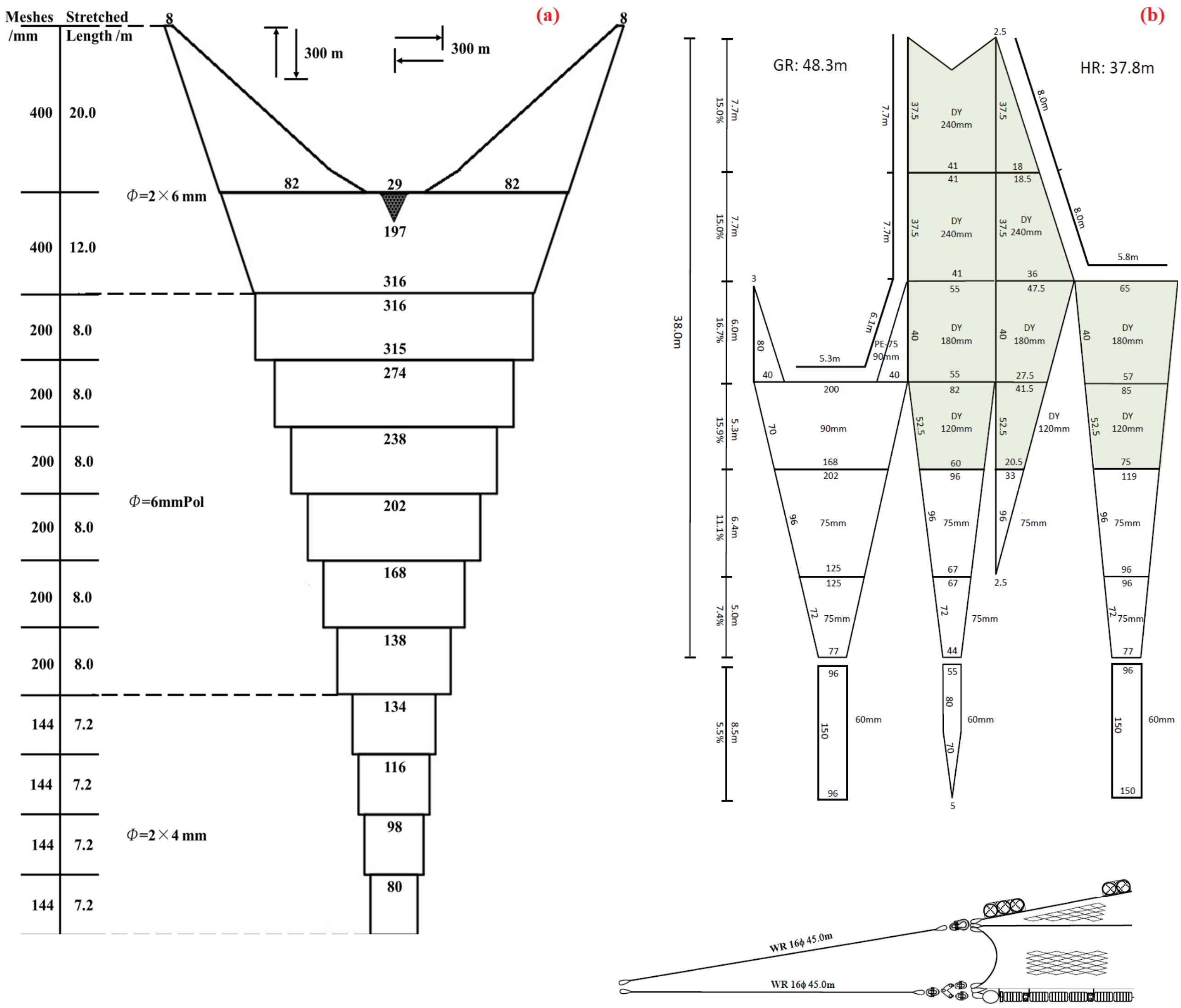

Figure 1. (a) Schematic net plan pelagic trawl and (b) net plan of the bottom trawl.

Table 1. Main specifications and parameters of the full-scale trawls and model trawls.

Trawls	C(m)	Tl(m)	Hl(m)	Fl(m)	F(kg)
Full-scale pelagic trawl	300	132.8	55.38	54.88	2146.2
Pelagic trawl model	8.848	3.85	1.59	1.568	0.15
Full-scale bottom trawl	81.6	46.5	37.8	48.6	249.48
Bottom trawl model	4.08	2.59	2.10	2.67	0.154

C, net opening circumference; Tl, trawl stretched length; Hl, headline length; Fl, fishing line length; F, buoyancy force.

2.2. Experiment Process in the Flume Tank

Flume tank experiments were carried out in the flume tank at Tokyo University of Marine Sciences and Technology (TUMSAT). The dimension of the test section of the tank was 9.0 m in length, 2.2 m in width, and 1.6 m in depth containing ~150 tons of freshwater. The flume tank was a horizontal and circular water channel, and the flow was driven by four contra-rotating impellers using constant-speed hydraulic delivery pumps with rated power of 132 Kw and delivering a flow speed that can be range 0~2 m/s. To reliably measure hydrodynamic forces and the mouth net high, the trawl models were attached to two vertical bars via the two bridles of 2.5 m each. The experiments were carried out in the flume tank by directly connecting the trawl's bridles to two bars connected to the masts of flume tank (tension meters) (Figure 3). The trawl model connection point contains a load cell, so that the frame-line tension at all connection points can be measured for each case. This load cell was A3064 manufactured by Electronic Industrial Co., Ltd with a maximum capacity of 10 kg and were amplified by a dynamic strain amplifer (DPM-6H). Then, these signals and the flow velocity signals were sent to an A/D converter and subsequently to a computer. The load cells were calibrated and zeroed at both the beginning and the end of each testing, and linearity was confirmed. A current meter was installed at approximately 2.0 m upstream of the trawl models to detect the flow velocity. Water density of the flume tank was 999.8 kg/m^3, and the water temperature was maintained at 17.6˚C ~18.4˚C during the experiments. Figure 2 shown the trawl net models in the flume tank. The bridle tensions of two trawl net were conducted at seven different towing speeds and five different door spreads (Table 2). As shown in Figure 2, the model trawls located at the middle of the flume tank for the case of pelagic trawl and the bottom as the case of bottom trawl and were free to move in the water flow. The two bars also ensured the horizontal opening of trawl model. The relationship between tension components measured during experiment and different forces can be determined from an angle θ between the bridle and flow direction as follow:

$$F_d = T\cos\theta \quad (1)$$

$$F_{in} = T\sin\theta/2 \quad (2)$$

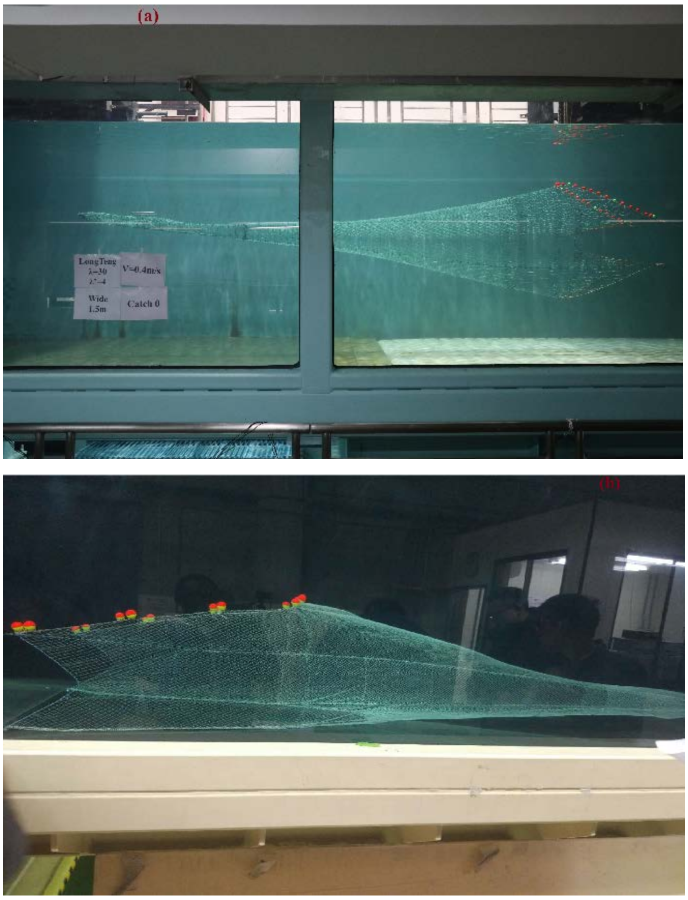

Figure 2. Trawl model in the flume tank: (a) Pelagic trawl and (b) Bottom trawl.

Table 2. The range of variables for model net test.

Variables	Pelagic trawl	Bottom trawl
Towing speeds (V)	0.29 m/s	0.57 m/s
	0.33 m/s	0.68 m/s
	0.38 m/s	0.8 m/s
	0.43 m/s	0.91 m/s
	0.47 m/s	1.02 m/s
	0.57 m/s	
	0.66 m/s	
Door spread	1.19 m	1.60 m
	1.36 m	1.80 m
	1.53 m	2.0 m
	1.70 m	
	1.85 m	

where F_d is the drag force; F_{in} is the in-pull force of trawl nets, and T is the bridle tension.

In this study the power consumption of the both trawls were calculated by multiplying the drag force and the towing speed (flow velocity in the flume tank) as:

$$P = F_d V \tag{3}$$

where F_d is the drag force; V is the flow velocity.

The energy efficiency is an important element that can be used to evaluate the engineering performance of the trawl net. The coefficient of energy consumption represents the energy consumed by the trawl net for unit volume of water filtered during the fishing operation and was calculated by the formula as following [17]:

$$C_{enf} = \frac{3.472 * F_{Td}}{H * Ws} \tag{4}$$

where F_{Td} is the total drag force of the trawl net system, H is the trawl net mouth height, and Ws is the wing-end spread.

2.3. Theorical Method to Calculate Trawl Net Parameters

2.3.1. Drag Calculation

It is presumable that the gear's string area plays a major role in its drag. The forms of various fishing nets are frequently more complicated than a flat netting panel, and the hydrodynamic properties of their individual netting sections might not be uniform. The premise that the resistance of a combined net of any shape is equal to the total of the drags of its netting components of simpler shape, regardless of their size or form, may be used to determine the estimated hydrodynamic resistance of fishing nets.

There are several formulas available to calculate the net drag in different ways some of the formulas which have been used are as follows:

Formula prescribed by Fridman for the calculation of hydrodynamic resistance of trawl is as follows [18]

$$R = C_x * q * A_t \tag{5}$$

where, R is the hydrodynamic resistance in kgf, C_x, is the hydrodynamic resistance coefficient derived from the angle of incidence and can be found in Fridmantable [18], A_t is twine Area and q: hydrodynamic stagnation pressure, calculated as follows:

$$q = p * \frac{V^2}{2} \tag{6}$$

with p the mass density of sea water in kgf·s^2·m^{-4} (105 kgf·s^2·m^{-4} for sea water), and V the flow velocity (m·s^{-1}), and A_t calculated using the following equation:

$$A_t = 4 * a * d * N \tag{7}$$

where d is twine diameter; a is bar length; N is the number of mesh in the trawl.

Reid (1977) [19] uses the following equation to describe a link between net drag, net speed, and net twine area that is independent of characteristics generated from the net geometry:

$$D = \frac{V^2 * A_t}{(54.72 * V + 115.2)} \tag{8}$$

where, D: drag in tons.

The MacLennan (1981) formula for calculation of net drag is [20]:

$$R_p = \frac{A_t * \left(\frac{61.2 + 46.6 * V^2}{1 + 0.0641 * V}\right)}{9807} \tag{9}$$

where, R_p is the net drag and V is the towing speed (knots).

The Nyatchouba *et al.* [5] formula for calculation of net drag is:

$$R_n = 82 * A_t * V^{1.561} \tag{10}$$

where R_n is the drag; V is the flow velocity; A_t is the twine area.

Zhou and Jiang in 1982 use Equation (11) to describe a link between net drag, flow velocity, and net twine area that is independent of characteristics generated from the net geometry [21]:

$$R_n = A_t * 24.9 * V^2 / (1 + 0.0516V) \tag{11}$$

To examine the changes in the estimated netting drag, all five formulae were used.

2.3.2. Net Mouth Height Calculation

It is important to estimate or predict the opening of the net for the pelagic and bottom trawls to get an idea of trawl shape and performance. Three formulas were used to predict the mouth opening.

The vertical opening of the gear by using Koyama *et al.* (1981) formula [22]:

$$H = 0.16 * a * V - 0.87 \tag{12}$$

where, H is vertical opening of mouth (m), a is the maximum circumference of the widest part of the belly (m), and V is the flow velocity (m/s).

Formulas given by Prado (1990) for the calculation of vertical and horizontal mouth opening of the net are as follows [23].

2.3.3. Vertical Opening

Formulas given by Prado (1990) for the calculation of vertical and horizontal mouth opening of the net are as follows:

$$VO = n * a(0.25 \text{ to } 0.3) \tag{13}$$

where VO is approximate vertical opening of net mouth (m), n is the width in number of meshes of front edge of belly, and a is mesh size (m).

The formula calculates the horizontal mouth opening of the net:

$$S \approx HR * 0.5(\text{to})0.60 \tag{14}$$

where S is horizontal opening of the trawl (Wing-end spread) in m spread and

HR is headline (m).

Formulas given by Nyatchouba *et al.* (2020a) for the calculation of net mouth height and wing-end spread are as follows [5]:

$$H_1 = 0.2514 * a * V^{-0.895} \tag{15}$$

where H_1 is the net mouth height; V is the flow velocity; a is the maximum circumference of belly part.

The wing-end spread can be expressed as follows:

$$W_s = 0.5506 e^{0.294 D_s} \tag{16}$$

where W_s is the wing-end spread; D_s is the door spread.

2.4. Data Analysis

Generalized linear models (GLMs) of drag and geometrical shape data were analyzed using Matlab software to estimate the impact of flow velocity and door spread on the trawl performance and compare the different formulation derived previously and the present experimental data. Thus, the performance parameter of trawl net such as drag force and net mouth height was fit as follows:

$$T_{per} = \alpha + \beta_1 M + \beta_2 V + \beta_3 D_s + \varepsilon \tag{17}$$

where the intercept is α, the terms β are regression coefficients, and the error term is ε. M represents the method or equations used, V represents the flow velocity (m/s), and D_s represents the door spread. A p-value greater than 0.05 was considered statistically significant. When terms were discovered to be non-significant, the term with the highest p-value was removed, and the model was refitted until all terms were significant.

3. Results and Discussion

3.1. Drag Force of the Two Flexible Trawl Nets

Drag forces of the both trawl nets from physical model tests and predicted formulas are shown in **Figure 3**. As present in **Figure 3(a)**, as the flow velocity increased from 0.28 to 0.66 m/s, the experimental drag force increased from 11.17 to 45.85 N. The measured drag force was about 23.05%, 31.51%, and 56.22% greater than the calculated drag force using the predict formulas of MacLennan in1981, Nyatchouba *et al.* in 2020, and Zhou and Jiang in 1982respectively, and the calculated drag force was 11.41% and 18.17%, respectively, greater than that from model tests. The measured drag force increased as flow velocity and door spread increases; It was 74.84% between the low and high flow velocities, 11.01% between the low and high door spreads (**Figure 3(a)**). However, as show in **Figure 3(b)**, the measured drag force of the bottom trawl net increased from 13.98 to 35.30 N as the flow velocity increased. This measured drag was 37.2%, 18.12%, and 1.37% lower than that obtained with the equation developed by Fridman (1986), Reid (1977), and MacLennan (1981), respectively, and was 17.27 and 41.45% greater than those obtained using the equations developed by Nyatchouba *et al.* (2020), and Zhou and Jiang (1982), respectively (Figure 3(b)). When the door spread is 2.0 m and 1.6 m, the measured drag forces of the bottom trawl are less than the drag force obtained at the door spread of 1.8 m.

GLM results (Table 3) describing the drag force of both trawl nets using experimental and analytical models explained 96.8% of the variability in the response variable (R^2). The most important factor affecting the drag force of both

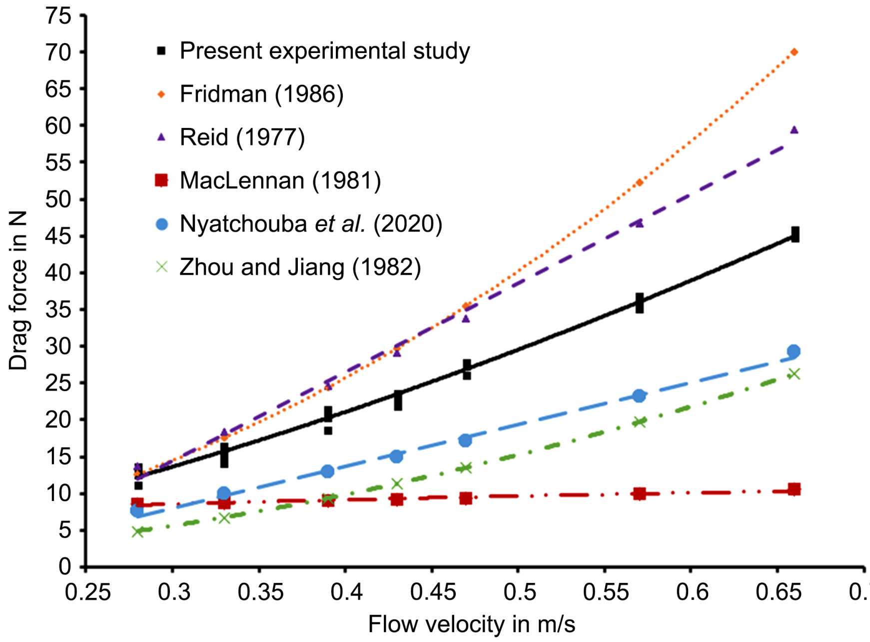

(a)

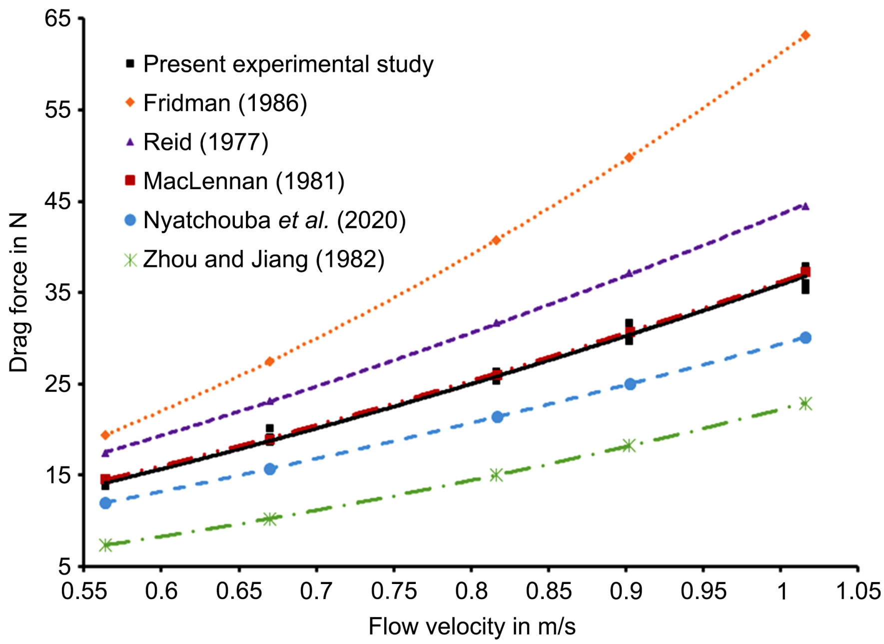

(b)

Figure 3. Drag force of the pelagic trawl net (a) and Bottom trawl net (b) obtained using experimental method and theorical methods in relation to flow velocity.

Table 3. The results of the GLM model explaining the variability in drag force of both trawls. V indicates the flow velocity (m/s) and D_s is the door spread (m).

Trawl model	Variable	Coefficient	Standard Error	*t*-Statistic	*p*-Value
Pelagic trawl net	Intercept	−16.862	1.366	−12.340	<0.001
	V	87.119	1.477	58.968	<0.004
	D_s	2.376	0.775	3.068	<0.001
	Present experiment model	25.72	10.95	233.121	<0.001
	Fridman (1986)	34.59	19.07	10.133	<0.001
	Reid (1977)	32.20	15.13	3.614	<0.001
	MacLennan (1981)	9.34	0.65	1.247	<0.001
	Nyatchouba *et al.* (2020)	16.42	7.11	3.012	<0.001
	Zhou and Jiang (1982)	13.13	7.07	81.457	<0.001
Bottom trawl	Intercept	−20.520	1.653	−12.413	<0.001
	V	49.408	0.846	58.373	<0.001
	D_s	3.613	0.836	4.323	<0.001
	Present experiment model	25.19	8.28	4.833	<0.001
	Fridman (1986)	40.15	16.13	58.33	<0.001
	Reid (1977)	30.77	9.97	44.25	<0.001
	MacLennan (1981)	25.54	8.38	27.60	<0.001
	Nyatchouba *et al.* (2020)	20.84	6.67	15.01	<0.001
	Zhou and Jiang (1982)	14.75	5.73	3.35	<0.001

trawl nets was flow velocity ($t = 58.968$, $p < 0.001$ and $t = 58.968$, $p < 0.001$ for pelagic and bottom trawls, respectively). Holding the other variables constant, a one-unit increase (by 0.1 m/s) in flow velocity would significantly increase the drag force by 9.11 N and 5 N for the pelagic and bottom trawls, respectively.

3.2. Power Consumption and the Coefficient of Energy Consumption of Two Flexible Trawl Nets

The power consumption was calculated by multiplying the drag force and flow velocity. As shown in **Figure 4(a)**, the power consumption of the pelagic trawl increased from 3.12 to 30.26 kW as the flow velocity increased from 0.28 to 0.66 m/s. At lower flow velocity, the experimental power from model tests was close to those obtained using the predicted drag equations with the gap less than 7%. While at the higher flow velocity, the power consumption obtained experimentally was 76.97%, 36.35%, and 42.83% greater than those calculated based on the

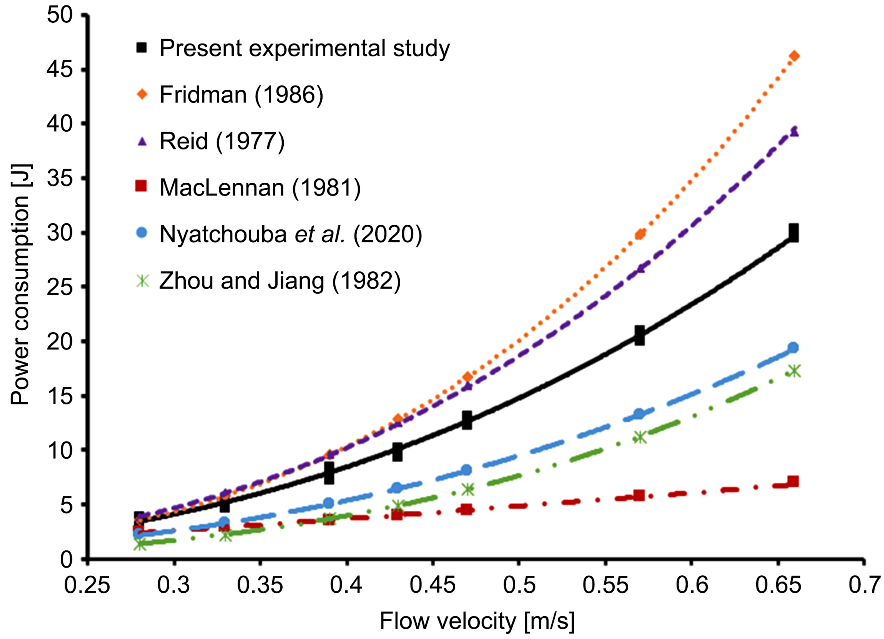

(a)

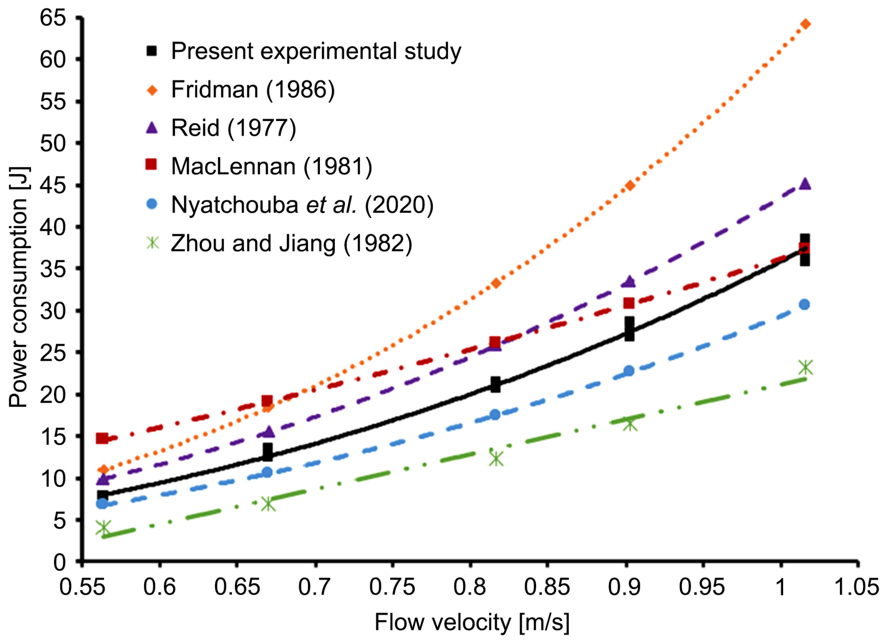

(b)

Figure 4. Power consumption of the pelagic trawl net (a) and Bottom trawl net (b) obtained using experimental method and theorical methods in relation to flow velocity.

predicted drag formulas of MacLennan (1981), Nyatchouba *et al.* (2020), and Zhou and Jiang (1982), respectively, and the calculated power consumption based on the drag formulas of Fridman (1986) and Reid (1977) was 34.56% and 22.78%, respectively, greater than that from model tests (**Figure 4(a)**). Increases in door spread lead to increases in power consumption; at the door spread of 1.85 m, the power of the pelagic model net was 17.49%, 7.46%, 2.97%, 2.24%

greater than that obtained at the door spread of 1.19 m. 1.36 m, 1.53 m, and 1.70 m, respectively. **Figure 4(b)** show that the power consumption of the bottom trawl increases from 7.88 to 35.86 KW as the flow velocity increase from 0.57 to 1.02 m/s. The experimental power consumption from model tests was 38.07%, 18.02%, and 16.69% lower than that obtained based on the model equations developed by Fridman (1986), Reid (1977), and MacLennan (1981), respectively, and was 17.38 and 40.80% greater than those obtained using the equations developed by Nyatchouba *et al*. (2020), and Zhou and Jiang (1982), respectively (**Figure 4(b)**). The power consumption of the bottom trawl obtained at the door spread of 2.0 m was 4.73% and 6.72% greater than that obtained at 1.8 and 1.6 m, respectively. That means that it recommended to towing the new-design pelagic trawl at the door spread of 1.53 - 1.85 m and for the new-design of bottom trawl at the door spread of 1.8 m.

The coefficient of the energy consumption of the pelagic trawl model in the flume tank increased from 0.059 to 0.34 kw·h/1000m^3 as the flow velocity increased from 0.28 to 0.66 m/s for all trawls tested (**Figure 6(a)**). The difference in coefficient of energy consumption is 36.10%, 30.80%, 59.71%, 26.56%, and 40.69 between the present experimental results and that using drag equations of Fridman (1986), Reid (1977), MacLennan (1981) Nyatchouba *et al*. (2020), and Zhou and Jiang (1982), respectively (**Figure 5(a)**). In comparison to the coefficients of energy consumption at door spreads of 1.19 m, 1.36 m, 1.53 m, and 1.70 m, respectively, the coefficient of energy consumption at the door spread of 1.85 m was 8.75%, 2.74%, 5.37%, and 3.04% lower. Demonstrating that as door distribution grows, overall energy efficiency increases (**Figure 5(a)**). However, **Figure 5(b)** indicates that more the flow velocity is higher, more the energy efficiency of the bottom trawl is lower with a variation of 6.80 to 36.64%. In average, the coefficients of energy consumption obtained in the present experimental study was 26.33, 2.86, 18.22 lower than that obtained using the predicted drag equation of Fridman (1986), Reid (1977), and Nyatchouba *et al*. (2020), respectively, and it was 14.5 and 50.21 greater than that obtained using the predicted drag equation of MacLennan (1981) and Zhou and Jiang (1982), respectively. The Coefficients of energy consumption obtained at the door spread of 1. 6m was about 0.03% and 18.73% greater than that obtained at 1.8 and 2.0 m, respectively (**Figure 5(b)**). The results indicate that towing the new-design bottom trawl at the door spread of 2.0 m would reduce the fuel consumption as used in Cameroonian fisheries.

3.3. In-Pull Force of the Two Flexible Nets

As flow velocity increases, the in-pull force of the pelagic trawl increases from 1.06 to 7.88 N (**Figure 6(a)**). The pelagic model trawl's mean in-pull forces were 2.24 N, 2.84 N, 3.47 N, 3.95 N, and 4.62 N at the door spread of 1.19 m, 1.36 m, 1.53 m, 1.70 m, and 1.85 m, respectively, which means that at 1.19 m, the size of the trawl door needed for a horizontal opening is 20.74%, 35.50%, 43.28%, and

51.48% smaller than that needed for a door spread of 1.36 m, 1.53 m, 1.70 m, and 1.85 m, respectively (**Figure 6(a)**). The measured in-pull forces were about 65.01%, 38.89%, and 51.22% greater than the calculated in-pull forces from the predicted drag formulas of MacLennan (1981), Nyatchouba *et al.* (2020), and Zhou and Jiang (1982), respectively, and the calculated in-pull forces from the

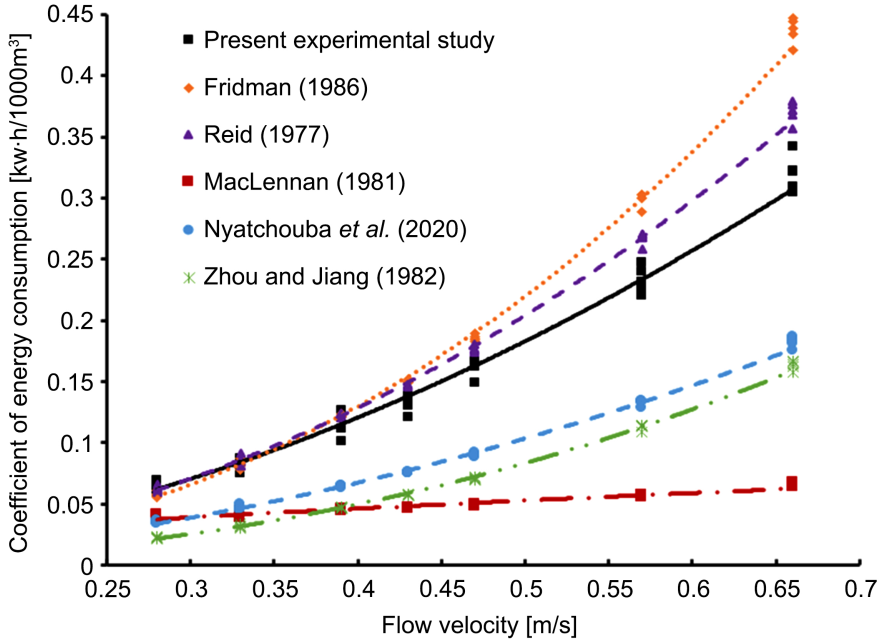

(a)

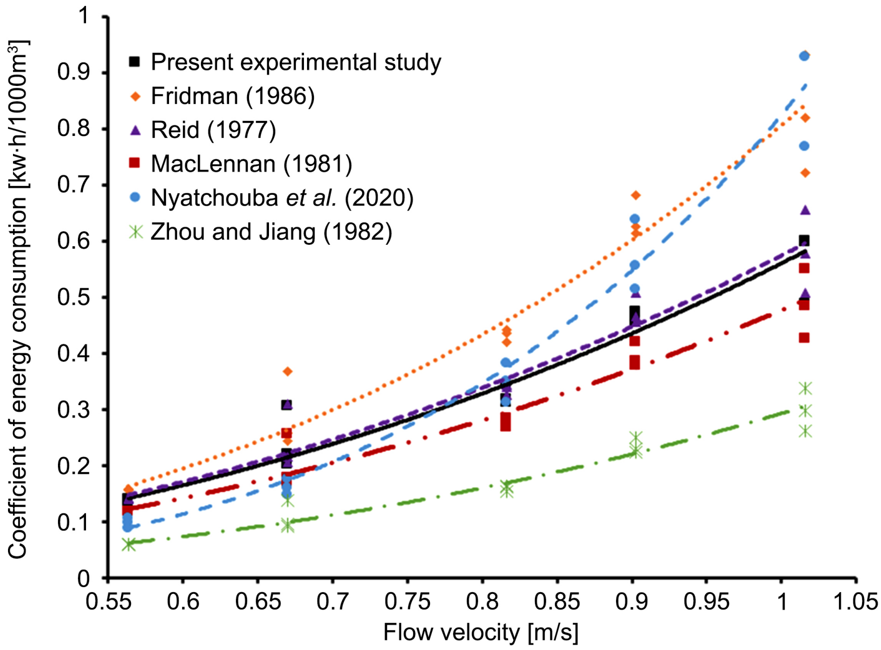

(b)

Figure 5. Coefficients of energy consumption of the pelagic trawl net (a) and Bottom trawl net (b) obtained using experimental method and theorical methods in relation to flow velocity.

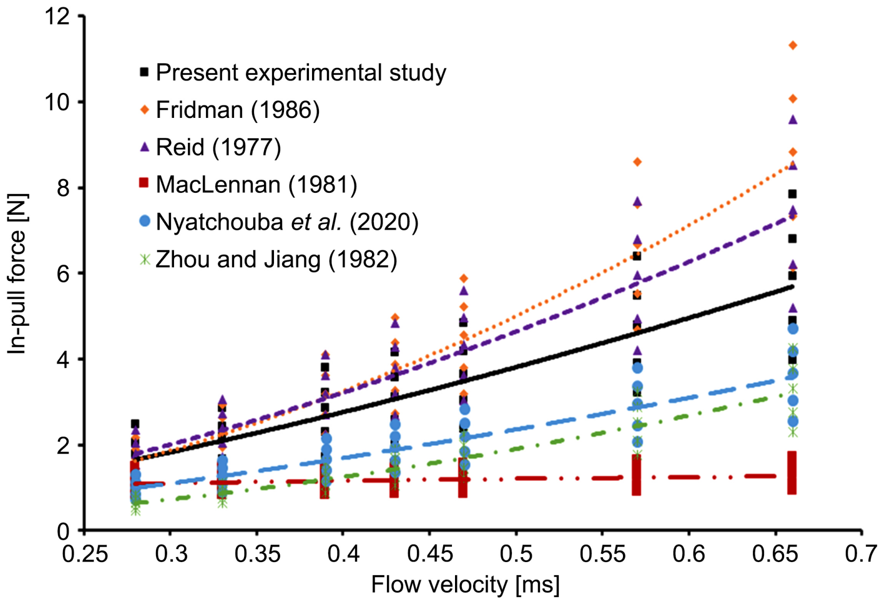

(a)

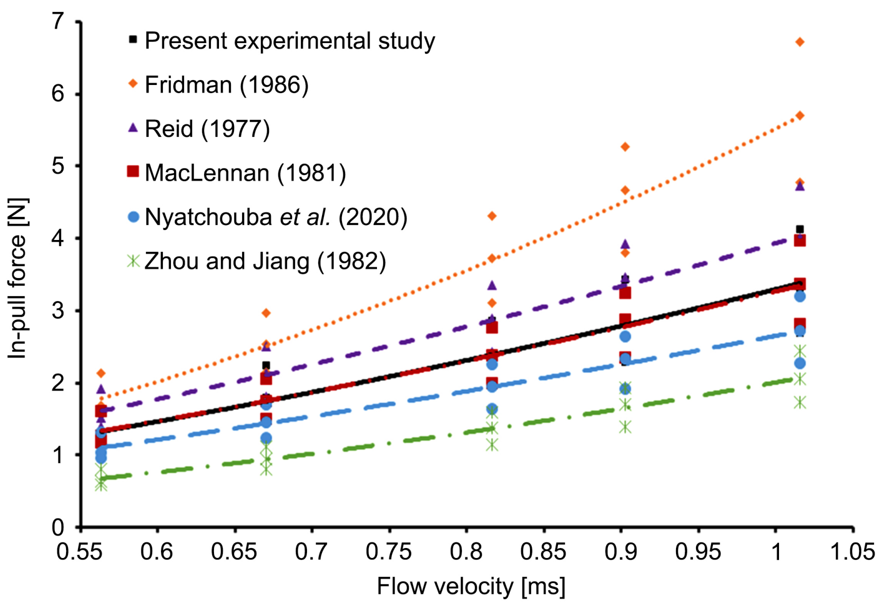

(b)

Figure 6. In-pull force of the pelagic trawl net (a) and Bottom trawl net (b) obtained using experimental method and theorical methods in relation to flow velocity.

drag formulas of Fridman (1986) and Reid (1977) was 22.21 and 16.53%, respectively, greater than that from model tests (**Figure 6(a)**). As shown in **Figure 6(b)**, an increase in flow velocity from 0.57 to 1.02 m/s led to an increase of the measured in-pull forces of bottom trawl model from 1.12 to 4.12 N. the statistical difference in-pull forces were less than 17.57% between the door spreads of 1.6 and 1.8 m, less than 18.49% between the door spreads of 1.8 and 2.0 m. The experimental in-pull force was 35.85 and 16.35 lower than that obtained from the drag formulas of Fridman (1986) and Reid (1977), respectively, while it was

0.75%, 19.02%, and 42.71% greater than that obtained from the drag formulas MacLennan (1981), Nyatchouba *et al.* (2020), and Zhou and Jiang (1982), respectively (Figure 6(b)).

3.4. Net Mouth Height of the Two Flexible Trawl Nets

Figure 7 shows the experimental predicted value of the height of net opening for both trawls. As can be seen from the result, the net mouth height of the pelagic

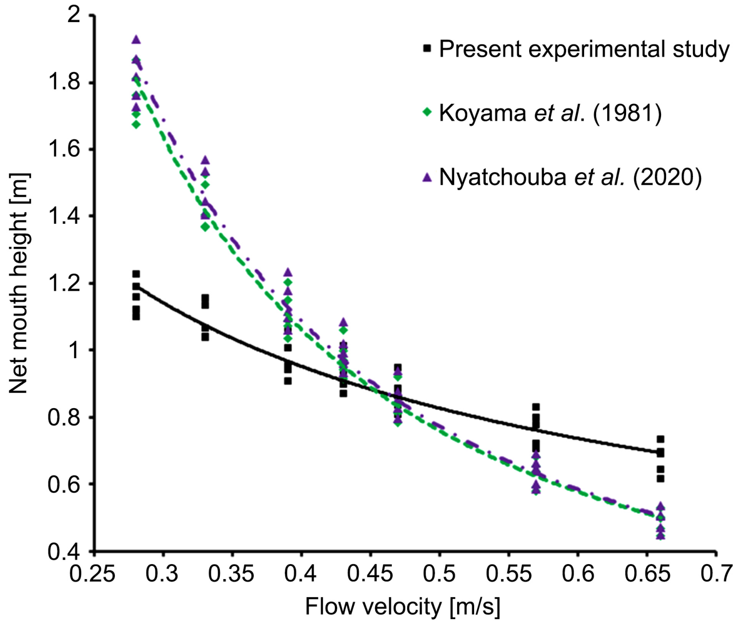

(a)

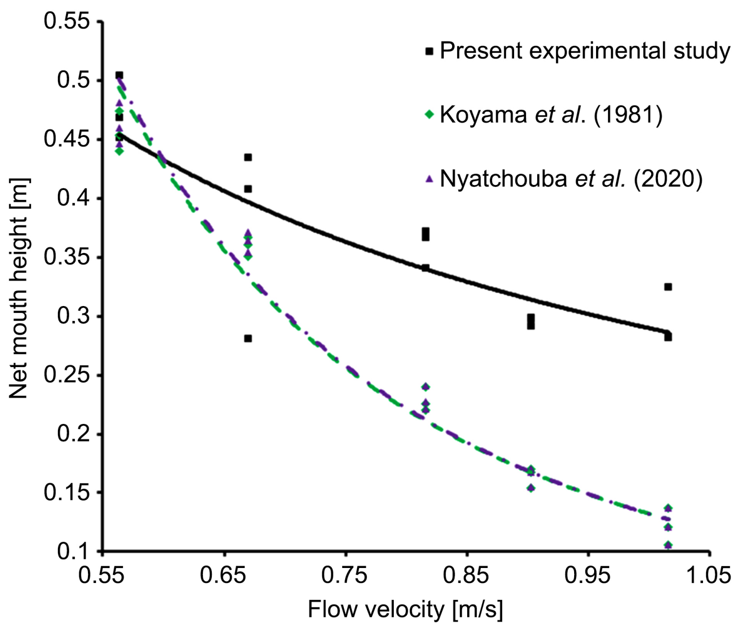

(b)

Figure 7. Net mouth height of the pelagic trawl net (a) and Bottom trawl net (b) obtained using experimental method and theorical methods in relation to flow velocity.

trawl decreased from 1.22 to 0.615 m, with the flow velocity increasing from 0.28 to 0.66 m/s. The variations in experimental net mouth height of were less than 12.11% and 5.85% between different flow velocity and door spreads, respectively. The calculated value using the predicted equations of Koyama *et al.* (1981) and Nyatchouba *et al.* (2020) was 10.75% and 12.85% greater than the experimental value, respectively (**Figure 7(a)**). As shown in **Figure 7(b)**, the measured values of the net mouth height of bottom trawl net varies with the flow velocity. Therefore, the higher the speed, the more the net mouth height decreases. At the slowest speeds (0.57 m/s), the net mouth height is greater than 0.50 m, while at the highest speed (1.02 m/s), the net mouth height of trawl net was about 0.29 m. When the door spread is 2.0 m, the trawls have a good net mouth height of 0.28 m on average unlike the door spreads of 1.6 m and 1.8 m. The calculated value using the predicted equations of Koyama *et al.* (1981) and Nyatchouba *et al.* (2020) was 26.27 and 25.62 lower than the experimental value, respectively (**Figure 7(b)**).

The results of the regression (**Table 4**) showed that the two variables (V and D_s) explained 92.7% of the variance observed ($p < 0.001$). The coefficients for flow velocity and door spread were negative, indicating that Net mouth height of both trawls decreased with increasing towing speed. More specifically, for every additional 0.1 m/s increase in flow velocity, et mouth height of both trawls decreased by 22.91%. Also increasing the door spread by 0.2 m generated a 6.61% decrease in Net mouth height of both trawls (**Table 4**).

Table 4. The results of the GLM model explaining the variability in net mouth height. V indicates the flow velocity (m/s) and D_s is the door spread (m).

Trawl model	Variable	Coefficient	Standard Error	*t*-Statistic	*p*-Value
Pelagic trawl net	Intercept	1.79	0.029	62.34	<0.001
	V	−1.27	0.031	−12.18	<0.004
	D_s	−0.19	0.016	−40.79	<0.001
	Present experiment model	0.93	0.17	103.32	<0.001
	Koyama *et al.* (1981)	1.03	0.42	39.091	<0.001
	Nyatchouba *et al.* (2020)	1.06	0.44	37.911	<0.001
Bottom trawl	Intercept	0.757	0.140	5.4	<0.001
	V	−0.380	0.072	−5.2	<0.001
	D_s	−0.053	0.071	−0.747	<0.001
	Present experiment model	0.36	0.076	10.068	<0.001
	Koyama *et al.* (1981)	0.27	0.129	40.52	<0.001
	Nyatchouba *et al.* (2020)	0.27	0.132	40.12	<0.001

3.5. Wing-End Spread of the Two Flexible Trawl Nets

The wing-end spread was strongly affected by flow velocity and door spread for both trawls (**Figure 8**). The measured wing-end spread of pelagic trawl increased from 0.58 to 0.88 m with the increases in flow velocity from 0.28 to 0.66 m/s (**Figure 8(a)**). On average, the door spread of 1.85 m produced the larger wing-end spread; it is 24.26%, 17.22%, 12.41%, and 4.68% higher than those

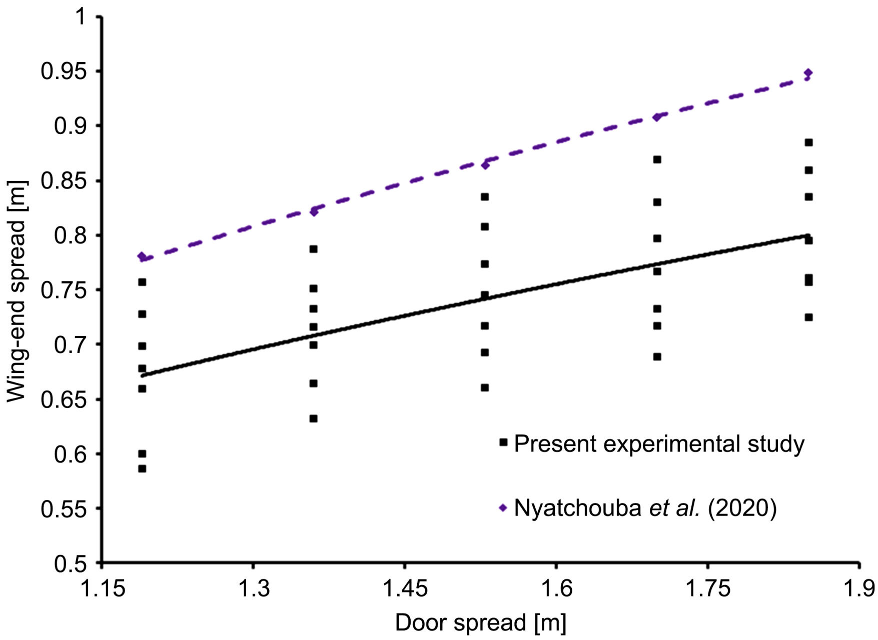

(a)

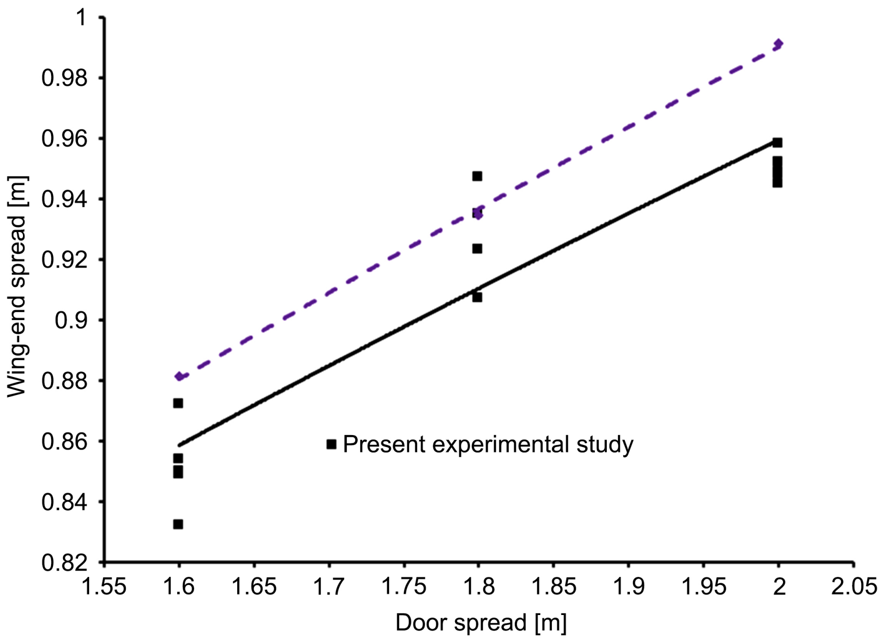

(b)

Figure 8. Wing-end spread of the pelagic trawl net (a) and Bottom trawl net (b) obtained using experimental method and theorical methods in relation to flow velocity door spread.

produced by the door spread of 1.19 m, 1.36 m, 1.53 m, and 1.70 m, respectively. These findings suggest that the pelagic trawl net will have a good horizontal opening the greater the door spread. The calculated values of the wing-end spread using the predicted equation of Nyatchouba *et al.* (2020) was greater than the experimental value in most cases with a maximum difference of about 23.57%. Overall, the mean difference was about 14.22% (**Figure 8(a)**). **Figure 8(b)** shown that the measured wing-end spread of bottom trawl increased from 0.832 to 0.49 m with the increases in flow velocity from 0.57 to 1.02 m/s. At the door spread increased, the measured wing-end spread of bottom trawl increased. Indeed, at the door spread of 2.0m the measured wing-end spread was 0.95 m; it was 10.41% and 2.46% greater than that obtained at the door spread of 1.6 and 1.8 m, respectively. The calculated values of the wing-end spread using the predicted equation of Nyatchouba *et al.* (2020) was 2.79% greater than the experimental value (**Figure 8(b)**).

3.6. Sweep Area of the Two Flexible Trawl Nets

The swept area of trawl is an important hydrodynamic performance index, which is generally considered to be directly proportional with the catch efficiency. Therefore, the swept area could only be roughly estimated. The experimental swept area was approximated by the product of the height of net opening and the horizontal distance between wing-ends and then multiplied by the shape coefficient (0.8). The measured swept area of pelagic trawl decreased from 0.75 to 0.36 m^2 with the increases in flow velocity from 0.28 to 0.66 m/s (**Figure 9(a)**). Averagely, the mouth area of the midwater trawl obtained at the door spread of 1.85 m was 11.31%, 5.65%, 6.92%, and 7.02% lower than that obtained at 1.19 m, 1.36 m, 1.53 m, and 1.70 m, respectively. The estimation value from model tests was lower than the calculated value from Nyatchouba *et al.* (2020) predicted equation, with a mean difference of about 43.85%. **Figure 9(b)** shows that the swept area of the bottom trawl model decreased from 0.43 to 0.23 m^2 as the flow velocity increased from 0.57 to 1.02 m/s, with the variation range from 0.74% to 9.44% between different flow velocities. The calculated value using the predicted equations of Nyatchouba *et al.* (2020) was 23.24% greater than the experimental value, respectively (**Figure 9(b)**).

4. Discussion

Cameroonian pelagic and bottom fishing grounds are abundant in resources, making them an important opportunity for the fishing industry and encouraging the development of efficient gear to reduce environmental impacts and protect ecosystems. In this study, two new trawl nets were designed based on target fishing vessels, and their hydrodynamic performances were investigated using a physical model and theoretical methods based on predicted equations proposed by various researchers. Between the flume tank measurements and the results obtained from different equations proposed by previous researchers such as

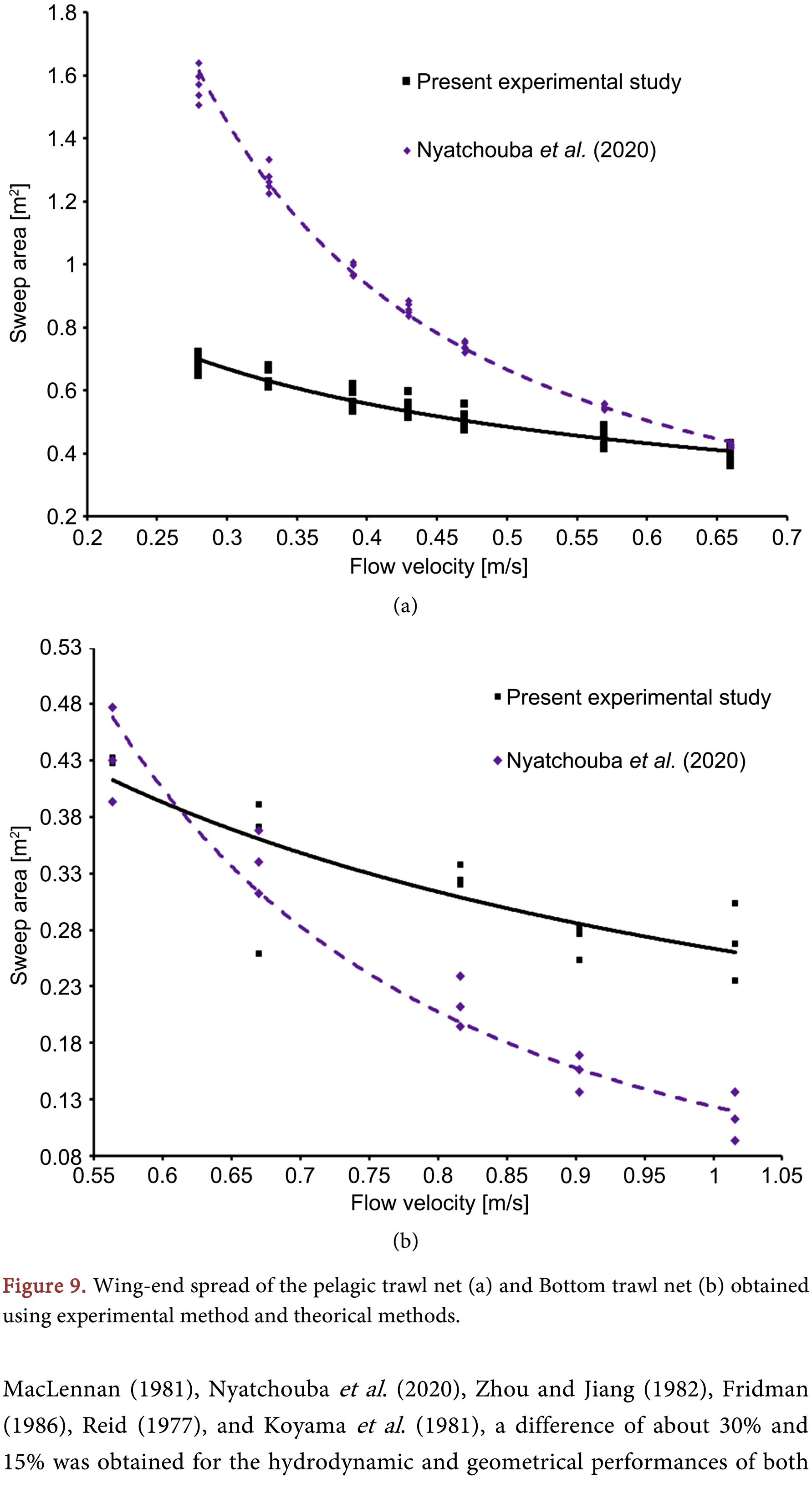

Figure 9. Wing-end spread of the pelagic trawl net (a) and Bottom trawl net (b) obtained using experimental method and theorical methods.

MacLennan (1981), Nyatchouba *et al.* (2020), Zhou and Jiang (1982), Fridman (1986), Reid (1977), and Koyama *et al.* (1981), a difference of about 30% and 15% was obtained for the hydrodynamic and geometrical performances of both trawl nets, respectively. Indicating that the theoretical method can be an alternative method on the determination of trawl net.

The newly designed pelagic trawl has a towing speed of 3.0 to 3.5 knots (0.47

to 0.57 m/s) and a door spread of 1.70 to 1.85 m (59.50 to 64.75 m). Under these conditions, the drag force of a pelagic trawl was approximately 27.24 to 36.73 N, the height of the net opening was approximately 0.71 to 0.89 m, and the wing-end spread was approximately 0.77 to 0.86 m in model scale. The swept area was approximately 0.56 to 0.76 m^2, and the drag per swept area was approximately 40.84 to 60.6 N/m^2, both of which were related to trawl net efficiency in terms of energy and catchability, *i.e.*, minimal drag (bridle tension) and maximum swept area [6] [24]. These conclusions were like those of Tang *et al.* [25] who modified the liner on the krill trawl net and analyze the effect of fishing operations parameter on the engineering performance of trawl net. Since the differences in drag between the different door spread is less than 11.5%, it is beneficial for the fishing vessel to use the maximum door spread at this towing speed to allow the midwater trawl net to have a very good performance during the trawling. For the case of new design bottom trawl net, the working towing speed that can be applied was 3.0 to 4.0 knots (corresponding to the full-scale towing speeds 4.051 to 4.77 m/s), and the appropriate door spread was about 1.8 m. In this case the drag force was about 25.51 to 30.43 N, the net mouth height of 0.31 to 0.38 m, and the wing-end spread of 0.91 m to 0.95m. These results agreed with those obtained by Nyatchouba *et al.* [6]. However, the swept area of the bottom trawl net under this condition was approximately 0.28 to 0.35 m^2, and the drag-to-swept-area ratio was 75.48 to 110.1 N/m^2, which was related to the trawl's energy and catch efficiencies [24]. The drag force of the trawl nets was designed to match the towing force of the trawlers used in Cameroonian fisheries. The working towing speed of 3.5 knots for pelagic trawls and 4.0 knots for bottom trawls would be suitable for harvesting the economically important species that we are concerned about, such as pelagic and demersal species, as mentioned in the introduction. Because of the large fish shoals, the height of the net opening is more important for pelagic trawl than bottom trawl, whereas the wing-end spread is more important for bottom trawl than pelagic trawl. Furthermore, the variation of the bottom trawl's net mouth height with flow velocity was less than that of pelagic trawls, whereas the variation of the bottom trawl's wing-end spread with flow velocity was greater than that of pelagic trawls. It was demonstrated in this study and in previous studiesthat the horizontal opening of both trawls depended on the door spread, whereas the vertical opening depended more on the towing speed and the floats for the bottom trawl, but the vertical opening also depended on the sinking forces for the pelagic trawl. After investigating the performance of the bottom trawl and pelagic trawl, we may investigate the effects of operation parameters and design parameters on trawl performance, such as mesh shape and twine material [5] [10]; cable length [26]; and the ratio of buoyancy to fishing line weight and sinking force [27]. This study proposed a bottom and pelagic trawl based firstly on the fishing vessel that operate in Cameroonian waters, on the different species that can be target, fishing ground, and carried out physical model test and theorical methods based on the predicted equations proposed previously using experimental models to explore the engineering performance of trawl net. This work may contribute to the standardization of industrial fisheries in Cameroon by improving the standardization of fishing gear management, such as bycatch reduction. Furthermore, its use would promote energy conservation, reduce gas emissions, and reduce the ecological impact of the fishing industry.

In this study, the formula developed by Zhou and Jiang (1982) based on two panel polyethylene bottom trawl nets, that propose by Nyatchouba *et al.* [5] using four trawl net design with four panel, and MacLennan (1981) based on four-panel polyethylene demersal trawl as a function of twine area and flow velocity provided a low prediction than the results obtained using the physical model test. This difference is probably because during our study, the trawl net models were constructed from only one twine material with four panel and experimental conditions compared to other trawl net. While the drag formulas of Fridman (1986) and Reid (1977) using based on four-panel and two panel polyethylene demersal and pelagic trawls are greater to the results of the physical model test. However, at the lower flow velocities and door spreads all the results obtained using the predicted equations were close to that obtained in the flume tank. Therefore, the use of the theorical methods based on the predicted equations proposed in this study to estimate the engineering performances of the both trawls are feasible.

The interaction between the trawl and the bottom was not considered in this study for the case of bottom trawl net. Furthermore, we believe that the complex interaction between the turbulent and fluttering motions of the trawl net should be studied for better trawl net performance, even though understanding it is difficult. However, fluttering motions, trawl deformation, and unsteady flow developing inside and around trawl nets can cause a reduction in trawl project area, warp vibrations, and influence the twine area, resulting in a change in the hydrodynamic performance of the trawl net [28]. Furthermore, numerical simulation can be used to analyze the engineering performance of trawl nets and provide accurate results when compared to the predicted equations used in this study, as well as obtain results that cannot be measured by physical model tests and sea trials [29]. This research provides the scientific foundation and guidance for the design of a trawl net, which will have numerous future applications in pelagic and demersal water fisheries.

5. Conclusions

We carried out investigations on the engineering performance of new-designed pelagic and bottom trawls for the fishing vessel that operates in Cameroonian water for application in pelagic and demersal fishing ground using physical model test and analytical method based on the published equations developed by some researchers using experimental data. The main conclusions are follows:

1) For both trawls, the drag forces, in-pull forces, power consumption, and

coefficient of energy consumption increased as the flow velocity and door spread increased, whereas the net mouth height and swept area decreased as the flow velocity increased. The trawl that we designed has superior hydrodynamic performance at 3.5 knots with a door spread of 1.85 m for pelagic trawl net and 3.0 knots with a door spread of 1.80 m for bottom trawl. This would be feasible and advantageous for the commercial fishing industries in Cameroonian waters.

2) The accuracy of the analytical method based on predicted equations used in this study for engineering performances of both trawls was confirmed by comparing analytical and experimental results, but the difference between these methods was greater when some equations were used. As a result, it was suggested that numerical simulation be used to replace the analytical methods used in this study because it can easily guide fishing gear design and carry out structural optimization explorations.

Acknowledgements

The authors are grateful for the "Allocation spéciale pour la modernisation de la recherche universitaire" from the Ministry of Higher Education (Cameroon). They are also grateful to Shanghai Ocean Universityfor the availability of the data made available to them, especially Prof. Liuxiong Xu and Prof. Hao Tang.

Conflicts of Interest

The authors declare no conflicts of interest regarding the publication of this paper.

References

[1] Nyatchouba, N.T.B., Kindong, R. and Xu, L. (2018) Reconstruction of Historical Fisheries Profile of Cameroon. *International Journal of Fisheries Science and Research*, **2**, 1008.

[2] Allerman, E. and Tilmans, W. (1985) Cosatal Conditions in West Africa: A Review. *Ocean and Coastal Management*, **19**, 199-240. https://doi.org/10.1016/0964-5691(93)90043-X

[3] Ssentongo, G. and Njock, J. (1987) Marine Fshery Resources of Cameroon: A Review of Exploited Fish Stocks. CECAF/ ECAF Series 87/44, FAO, Rome. http://www.fao.org/docrep/003/s4639e/S4639E00.htm#TOC

[4] Belhabib, D., Hellebrandt, D., Edward, E. and Pauly, D. (2015) Reconstructing Fisheries Catches for Cameroon between 1950 and 2010. Sea around Us, Fisheries Centre, University of British Columbia, Vancouver, 10.

[5] Nyatchouba, N.T.B., Tang, H., Xu, L., You, X., Hu, F., Njomoue, P.A. and Kindong, R. (2020) Hydrodynamic Performance of Bottom Trawls with Different Materials, Mesh Sizes and Twine Thicknesses. *Fisheries Research*, **221**, Article ID: 105403. https://doi.org/10.1016/j.fishres.2019.105403

[6] Nyatchouba, N.T.B., Tang, H., Njomoue, P.A., Xu, L., Hu, F. and You, X. (2020) Comparative Study on the Full-Scale Prediction Performance of Four Trawl Nets Used in the Coastal Bottom Trawl Fishery by Flume Tank Experimental Investigation. *Applied Ocean Research*, **95**, Article ID: 102022. https://doi.org/10.1016/j.apor.2019.102022

[7] Njomoue, P.A., Nyatchouba Nsangue, B.T., Ngatcha, N.A., N'Souvi, K., *et al.* (2020) Predictive Models for Codend Size Selectivity for the Arioma Bondi Silver-Rag Driftfish (Ariommatidae) in the Cameroonian Bottom Trawl Fisheries: Effects of Mesh Size on the Size Selection. *International Journal of Fisheries and Aquatic Research*, **5**, 13-22.

[8] Lee, J., Lee, C.-W., Songho, P., Jieun, K., Subong, P. and Taeho, K. (2018) Development of a Low-Energy Midwater Trawl with Different Combinations of Trawl Nets and Trawl Doors through Model Experiments. *Fisheries Science*, **84**, 323-334. https://doi.org/10.1007/s12562-017-1158-1

[9] Nyatchouba Nsangue, B.T., Tang, H., Xu, L. and Hu, F. (2019) Effect of Mesh Size, Twine Material and Trawl Gear Accessories on the Bottom Trawls Hydrodynamic Performance. *International Journal of Fisheries and Aquatic Research*, **4**, 1-9.

[10] Sterling, D. and Balash, C. (2017) Engineering and Catching Performance of Five Netting Materials in Commercial Prawn-Trawl Systems. *Fisheries Research*, **193**, 17-24. https://doi.org/10.1016/j.fishres.2017.04.014

[11] Hu, F., Matuda, K., Tadashi, T. and Haruyuki, K. (1995) Dynamic Analysis of Midwater Trawl System by a Two-Dimensional Lumped Mass Method. *Fisheries Science*, **61**, 229-233. https://doi.org/10.2331/fishsci.61.229

[12] Feng, C., Liu, J., Zhang, Y., Wang, Y., Zhang, X., Zhou, A., Wang, L. and Wang, L. (2017) Structure Improvement Design and Performance Experiment of Antarctic Krill Trawl Net. *Transactions of the Chinese Society of Agricultural Engineering*, **33**, 75-81. (In Chinese with English Abstract)

[13] Wan, R., Jia, M., Guan, Q., Huang, L., Cheng, H., Zhao, F., He, P. and Hu, F. (2019) Hydrodynamic Performance of a Newly-Designed Antarctic Krill Trawl Using Numerical Simulation and Physical Modeling Methods. *Ocean Engineering*, **179**, 173-179. https://doi.org/10.1016/j.oceaneng.2019.03.022

[14] Winger, P.D., DeLouche, H. and Legge, G. (2006) Designing and Testing New Fishing Gears: The Value of a Flume Tank. *Marine Technology Society Journal*, **40**, 44-49. https://doi.org/10.4031/002533206787353240

[15] Nyatchouba, N.T.B., Tang, H., Achille, N.P., Xu, L. and Hu, F. (2022) Unsteady Turbulent Flow Developing Inside and around Different Parts of Fluttering Trawl Net in Flume Tank. *Journal of Fluids and Structures*, **108**, Article ID: 103451. https://doi.org/10.1016/j.jfluidstructs.2021.103451

[16] Hu, F., Matuda, K. and Tokai, T. (2001) Effects of Drag Coefficient of Netting for Dynamic Similarity on Model Testing of Trawl Nets. *Fisheries science*, **67**, 84-89. https://doi.org/10.1046/j.1444-2906.2001.00203.x

[17] Xu, L.X. (2004) Fishing Gear Theory and Design. China Agriculture Press, Beijing. (In Chinese)

[18] Fridman, A.L. (1986) Calculations for Fishing Gear Designs. Arrangement with the Food and Agriculture Organization of the United Nations by Fishing News, Farnham.

[19] Reid, J.A. (1977) A Net Drag Formula for Pelagic Nets. Scottish Fisheries Research. Report No. 7.

[20] MacLennan, D. (1981) The Drag of Four-Panel Demersal Trawls. *Fisheries Research*, **1**, 23-33. https://doi.org/10.1016/0165-7836(81)90004-7

[21] Zhou, Y.Q. and Jiang, Z.Z. (1982) Study on Drag Characteristics of Trawl Nets and a Method for the Calculation Trawl Net Drag. Selected Papers Presented to the Marine fishing Academic Seminar. Chinese Society of Fisheries, Beijing, 82-92.

[22] Koyama, *et al.* (2008) Drag and Sheer of the Suberkrub Type of Trawl Boards. *Bulletin of the National Research Institute of Fisheries Engineering*, **2**, 95-103.

[23] Prado, J. (1990) Fisherman's Workbook. FAO, Fishing News Books, Blackwell Scientific Publications Ltd., Oxford.

[24] Priour, D. (2009) Numerical Optimization of Trawls Design to Improve Their Energy Efficiency. *Fisheries Research*, **98**, 40-50. https://doi.org/10.1016/j.fishres.2009.03.015

[25] Tang, H., Nsangue, B.T.N., Pandong, A.N., He, P., Liuxiong, X. and Hu, F. (2022) Flume Tank Evaluation on the Effect of Liners on the Physical Performance of the Antarctic Krill Trawl. *Frontiers in Marine Science*, **8**, Article 829615. https://doi.org/10.3389/fmars.2021.829615

[26] Khaled, R., Priour, D. and Billard, J.Y. (2013) Cable Length Optimization for Trawl Fuel Consumption Reduction. *Ocean Engineering*, **58**, 167-179. https://doi.org/10.1016/j.oceaneng.2012.10.001

[27] Feng, C.L., Huang, H.L., Zhou, A.Z., Zhang, X., Liu, J., Xu, G.D. and Chen, X.Z. (2012) Performance Optimization of a Trawl for Antarctic Krill. *Journal of Fishery Sciences of China*, **19**, 662-670. (In Chinese with English Abstract).

[28] Druault, P. and Germain, G. (2016) Analysis of Hydrodynamics of a Moving Trawl Codend and Its Fluttering Motions in Flume Tank. *European Journal of Mechanics—B/Fluids*, **60**, 219-229. https://doi.org/10.1016/j.euromechflu.2016.06.010

[29] Nguyen, T.X., Winger, P.D., Orr, D., Legge, G., DeLouche, H. and Gardner, A. (2015) Computer Simulation and Flume Tank Testing of Scale Engineering Models: How Well Do These Techniques Predict Full-Scale At-Sea Performance of Bottom Trawls? *Fisheries Research*, **161**, 217-225. https://doi.org/10.1016/j.fishres.2014.08.007